JBC RESEARCH ARTICLE

YibN, a *bona fide* interactor of the bacterial YidC insertase with effects on membrane protein insertion and membrane lipid production

Received for publication, December 16, 2024, and in revised form, February 23, 2025 Published, Papers in Press, March 11, 2025,
https://doi.org/10.1016/j.jbc.2025.108395

Zhiyu Zhao[1], Nachi Yamamoto[2], John W. Young[1], Nestor Solis[3], Amos Fong[1], Mohammed Al-Seragi[1], Sungyoung Kim[4], Hiroyuki Aoki[4], Sadhna Phanse[4], Hai-Tuong Le[1], Christopher M. Overall[3,5], Hanako Nishikawa[2], Mohan Babu[4], Ken-ichi Nishiyama[2], and Franck Duong van Hoa[1,*]

From the [1]Department of Biochemistry and Molecular Biology, Faculty of Medicine, Life Sciences Institute, University of British Columbia, Vancouver, British Columbia, Canada; [2]Department of Applied Biochemistry and Food Science, Faculty of Agriculture, Iwate University, Morioka, Iwate, Japan; [3]Department of Oral Biological and Medical Sciences, Centre of Blood Research, Life Sciences Institute, University of British Columbia, Vancouver, British Columbia, Canada; [4]Department of Biochemistry, Faculty of Science, University of Regina, Canada; [5]Yonsei Frontier Lab, Yonsei University, Seoul, Republic of Korea

Reviewed by members of the JBC Editorial Board. Edited by George M. Carman

YidC, a prominent member of the Oxa1 superfamily, is essential for the biogenesis of the bacterial inner membrane, significantly influencing its protein composition and lipid organization. It interacts with the Sec translocon, aiding the proper folding of multi-pass membrane proteins. It also functions independently, serving as an insertase and lipid scramblase, augmenting the insertion of smaller membrane proteins while contributing to the organization of the bilayer. Despite the wealth of structural and biochemical data available, how YidC operates remains unclear. To investigate this, we employed proximity-dependent biotin labeling (BioID) in *Escherichia coli*, leading to the identification of YibN as a crucial component within the YidC protein environment. We then demonstrated the association between YidC and YibN by affinity purification-mass spectrometry assays conducted on native membranes, with further confirmation using on-gel binding assays with purified proteins. Co-expression studies and *in vitro* assays indicated that YibN enhances the production and membrane insertion of YidC substrates, such as M13 and Pf3 phage coat proteins, ATP synthase subunit c, and various small membrane proteins like SecG. Additionally, the overproduction of YibN was found to stimulate membrane lipid production and promote inner membrane proliferation, perhaps by interfering with YidC lipid scramblase activity. Consequently, YibN emerges as a significant physical and functional interactor of YidC, influencing membrane protein insertion and lipid organization.

Membrane proteins (MPs) constitute approximately 20 to 25% of the cellular proteome and are essential for various functions, including signal transduction, nutrient transport, and energy production (1). Their proper assembly into the lipid bilayer is critical for maintaining membrane functionality. In *Escherichia coli*, the insertion of MPs into the membrane relies on the Sec translocon (2, 3). This machinery consists of the core SecYEG complex, which forms the membrane channel for protein translocation, along with additional factors such as the SecDFYajC sub-complex, the SecA ATPase, the YidC insertase and several other accessory components (4–7). Together, these components ensure the proper insertion and folding of MPs within the lipid bilayer, thereby upholding the integrity of the membrane bilayer in both form and function.

While YidC has a pivotal role in the biogenesis of multi-pass membrane proteins *via* the Sec translocon, it also functions in a Sec-independent manner to help the insertion of small membrane proteins (8, 9). YidC is a member of the conserved YidC/Alb3/Oxa1 insertase family, functioning within the bacterial, thylakoidal, and mitochondrial inner membranes, respectively, to facilitate the insertion of crucial components into energy-transducing complexes (10, 11). This includes the F_1F_0 ATP synthase subunit c (F_0c) vital for ATP production. Additionally, in bacteria, YidC plays a role in the insertion of phage coat proteins M13 and Pf3, mechanosensitive channel subunits such as MscL, and components of the type VI secretion system like TssL (12–15). Despite the established importance of YidC in these processes, further research is required to elucidate the mechanisms by which the insertase facilitates the incorporation of small membrane proteins into the lipid bilayer.

Protein interactions and co-regulations offer critical insights into underlying molecular mechanisms, often explained by the guilt-by-association principle (16, 17). An illustrative example is the use of chemical cross-linkers, which revealed that the protease FtsH and its regulatory partners, HflC and HflK, are in proximity to YidC, thereby emphasizing the importance of protein quality control in YidC-mediated membrane insertion (18, 19). Investigation into YidC depletion also revealed a co-regulation of a specific glycolipid, termed MPIase (20). This

* For correspondence: Franck Duong van Hoa, Fduong@mail.ubc.ca.
Present address for John W. Young: Department of Chemistry, Kavli Institute for Nanoscience Discovery, Dorothy Crowfoot Hodgkin Building, University of Oxford, South Parks Road, Oxford.

glycolipid was subsequently shown to significantly enhance the insertion efficiency of various small membrane proteins, including F_0c and phage proteins Pf3 and M13 (21, 22). Thus, knowledge of interaction networks can inform and help elucidate complex biological processes.

In this study, utilizing proximity-dependent biotin labeling (BioID) (23), we identify YibN, a 16 kDa single-pass inner membrane protein oriented towards the cytosol. We validate the YidC-YibN interaction *in vitro* and confirm its reliance on an intact N-terminal transmembrane segment. While YibN is not essential for cell viability, its expression significantly enhances the production of various small membrane proteins, including M13 procoat (PC-Lep), Pf3 (Pf3-23Lep), and F_0c, as well as SecG. These latter findings are supported by *in vitro* protein translation and insertion assays. Additionally, the overproduction of YibN also correlates with increased membrane lipid synthesis and inner membrane proliferation, and recent studies have indicated that lipid scrambling and bilayer reorganization are linked to membrane insertase activity (24, 25). These findings together place YibN as a *bona fide* interactor of YidC.

Results

Identifying potential interactors of YidC using BioID

The mutant biotin ligase BirA* (BirA R118G) (23) was fused to the C-terminus of YidC on plasmid pBAD22 (Fig. S1). After protein expression, the bacterial inner membrane was isolated and solubilized with 1% DDM. The extracted proteins were visualized on SDS-PAGE and those biotinylated were detected by Western Blot (Fig. 1*A*). As expected, many proteins were biotinylated with YidC-BirA* compared to YidC-BirA, and none with YidC (right panel, Fig. 1*A*). The detergent extract was also incubated with NeutrAvidin beads to isolate the biotinylated proteins. The eluted proteins were trypsin-digested and analyzed by LC-MS/MS. A total of 172 proteins were detected across four replicates, with 21 proteins found in common across the replicates (File S1). The proteins identified were ranked based on their spectral counts and plotted in Figure 1*B*. As expected, YidC and BirA were efficiently detected in the samples. The protein BCCP (gene name: *accB*), the natural substrate of BirA, was also identified with a high spectral count. Other proteins, such as FtsH, HflK, and HflC, previously reported vicinal to YidC based on chemical cross-linking analysis (18), were also efficiently detected. Strikingly, the protein with the highest spectral counts, and consistently across four replicates, was the uncharacterized protein YibN.

Validation of YibN-YidC interaction using affinity pulldown

Recombinant His-tagged YidC and control empty plasmid pBAD22 were transformed into strain JW2806 to allow SILAC-labeling with Lys4/Lys0 lysine isotopologues. After YidC expression, the membrane fraction was solubilized with DDM and incubated with Ni-NTA agarose beads. After washing, the proteins retained with YidC were identified by LC-MS/MS (Fig. 1*C*). As expected, His-tagged YidC was well detected in the sample, with >150-fold enrichment over the background. Strikingly, endogenously expressed YibN was also detected, with >20-fold enrichment over the background. In the reciprocal experiment, His-tagged YibN and the control empty plasmid were transformed into strain JW2806. Recombinant YibN was enriched in the sample (>20-fold), and endogenous YidC was also well detected (>50-fold over the background; Fig. 1*D*). The pulldown experiments were then conducted with the recombinant strain B3611 (26). In this strain, the chromosomally encoded YibN protein is tagged at the C-terminus with a peptide affinity SPA tag (16, 27). The untagged parental strain DY330 was employed as a control to subtract non-specific binding to the FLAG resin. The data, plotted in Figure 1*E*, show that YidC and YibN are the two most abundant proteins isolated from strain B3611 under native expression conditions.

Validation of the YidC-YibN interaction by native-gel electrophoresis

His-tagged YidC and His-tagged YibN were purified to homogeneity in DDM detergent. The proteins were analyzed by SDS-PAGE (left panel, Fig. 1*F*) and blue-native PAGE (right panel, Fig. 1*F*). The blue-native gel analysis revealed that YidC and YibN form a distinctive band when incubated together (labeled YY in Fig. 1*F*). To confirm the identity of this band, the YibN transmembrane segment (TMS; residue 1–29) was deleted. On the blue-native PAGE, the truncated Δ1 to 29 YibN failed to associate with YidC, indicating that the TMS of YibN is essential for the formation of the YidC-YibN complex.

YibN overexpression leads to inner membrane proliferation

During the YibN purification procedure on a sucrose gradient, we noticed that a larger amount of inner membrane is produced compared to the control plasmid strain (left panel, Fig. 2*A*). Total membrane lipids were extracted and analyzed by thin-layer chromatography (TLC; right panel, Fig. 2*A*). This analysis confirmed that the YibN overproducing strain produced ∼4-fold more membrane lipids than the control strain, with phosphatidylethanolamine (PE) and phosphatidylglycerol (PG) remaining the predominant species. The same cells were also stained and visualized by transmission electron microscopy. The images show that YibN production is associated with membrane proliferation, circumvolutions and multilayered structures principally at the level of the bacteria's inner membrane (compare Fig. 2, *B* and *C*). The overall shape of the outer membrane seems less affected (Fig. S2).

YibN augments the biogenesis of YidC substrates

We tested the effect of YibN on three known YidC substrates: M13 procoat (PC) and Pf3 coat proteins, each fused to the soluble domain of leader peptidase (Lep) to facilitate their detection (28, 29), and F_1-F_0 subunit F_0c (13). These substrates were co-expressed with YibN or the control empty plasmid pBAD33 (Fig. 3) in the BL21 (DE3) strain at room temperature using 0.1% arabinose for 15 min, followed by the addition of 0.75 mM IPTG to induce substrate synthesis. Aliquots were collected every 15 min for analysis by SDS-PAGE and Western

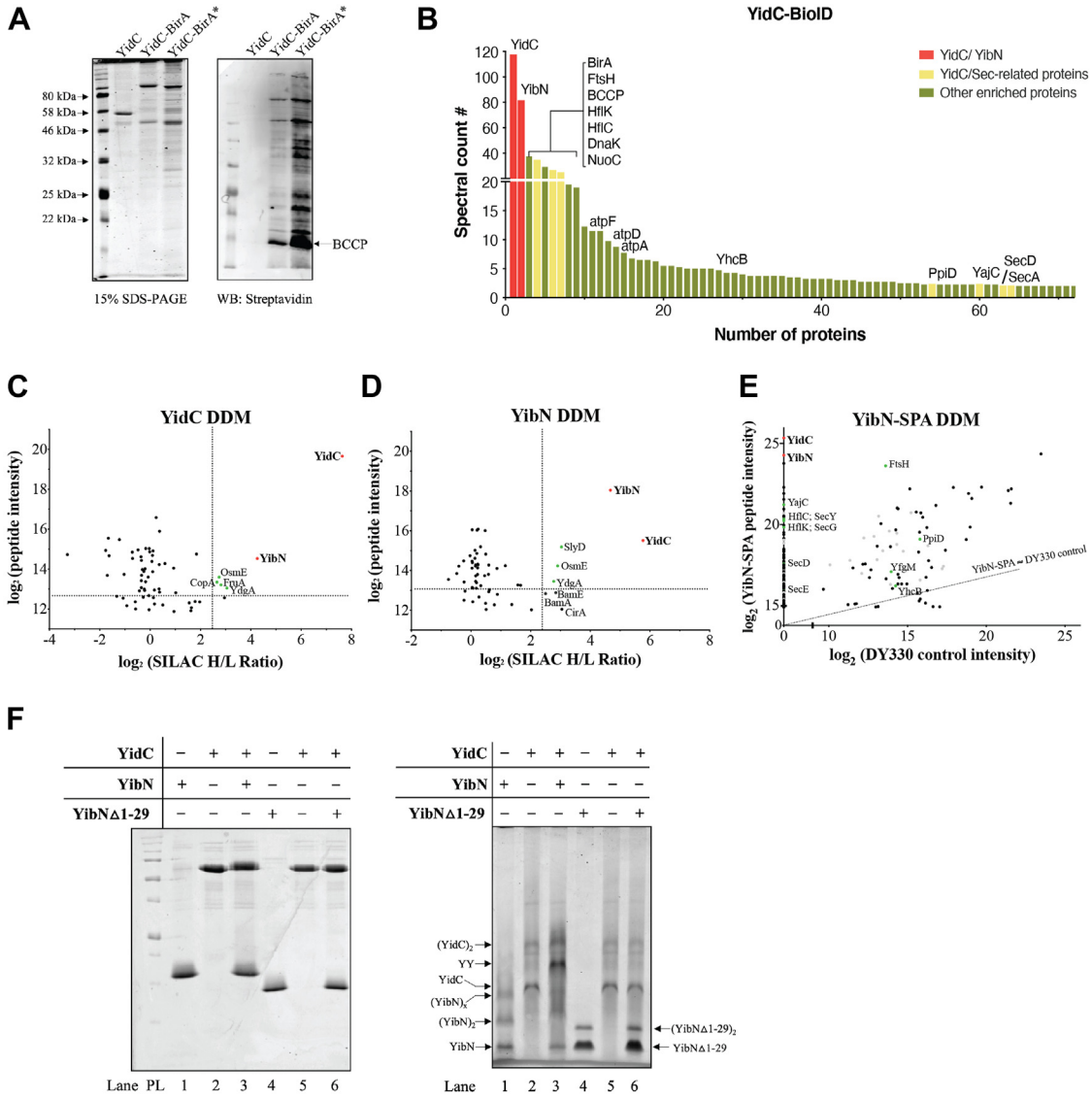

Figure 1. Identification and validation of the YidC-YibN interaction. *A*, BirA* was fused to the C-terminus of YidC. Expression of the fusion protein YidC-BirA* allows biotinylation in *E. coli*. Following the inner membrane vesicle (IMV) isolation and solubilization in detergent DDM, the biotinylated proteins were pulled down *via* streptavidin resin. The eluted proteins are analyzed on SDS-PAGE and Western Blot. The aliquots of IMVs of YidC-BirA* and its controls YidC-only and YidC-BirA are loaded onto 15% SDS-PAGE followed by Coomassie staining. The biotinylation was verified on Western Blot (Streptavidin anti-biotin). *B*, top hits of YidC-BioID identified by LC-MS/MS. YidC and YibN are highlighted in *red*. YidC/Sec-related proteins (reported interacting with YidC or in the vicinity of YidC: van Bloois *et al.*, 2008; (58); Young *et al.*, 2022) are labeled in *yellow*. "Other enriched proteins" are labeled in *green*. *C* and *D*, validation of YibN-YidC interaction by AP-MS. SILAC-AP/MS was conducted in detergent DDM. The crude membranes containing either (*C*) YibN-$_{His6}$ or (*D*) $_{His6}$-YidC obtained from Lys4-labeled *E.coli* JW2806 strain were solubilized in 0.8% DDM followed by Ni-NTA purification. Empty vector pBAD33 or pBAD22 were used as controls and expressed in Lys0-labeled media. The $\log_2$(peptide intensity) of each protein identified in the pull-down assay was plotted against its corresponding $\log_2$(SILAC H/L ratio). The proteins with an H/L ratio larger than 5 ($\log_2$(SILAC H/L ratio) $>$ 2.4) will be considered "enriched". The y-axis cutoff was set to the $\log_2$(peptide intensity) point, where three-quarters of data points will be above this cutoff. YidC/YibN are highlighted in *red*. Proteins with $\log_2$(SILAC H/L ratio) larger than 2.4 and top 75% abundant proteins are labeled in *green*. *E*, endogenous YibN-SPA pull-down assay. *E. coli* strain B3611 bearing SPA-tagged YibN was grown. The pull-down assay was conducted in detergent DDM. YidC and YibN are labeled in *red*. Known interactors of YidC (van Bloois *et al.*, 2008; (58), 2017; Young *et al.*, 2022) are labeled in green. Ribosomal proteins are labeled in *grey*. Proteins between YibN and YajC are GntR, YgfX, QmcA, and CorA. *F*, biochemical evidence of YidC and YibN complex. YidC, YibN, and YibNΔ1 to 29 sample analysis on SDS-PAGE (containing β-ME), followed by Coomassie Blue staining (*left panel*). YidC-YibN binding analysis on BN-PAGE. 3 μg of YibN, YidC or YibN Δ1 to 29 were loaded as indicated.

Blot with the corresponding detection antibodies. The overall bacterial growth rate and cell protein content remained unchanged when the substrates were co-expressed with YibN or the empty plasmid (Fig. S3, *A*–*C*). However, the synthesis of PC-Lep, Pf3-23Lep, and F_0c was significantly increased in the presence of YibN (Fig. 3, *A*–*C*). These co-expression experiments were also conducted with three other small membrane proteins, SecG, YajC, and YhcB (Figs. 3*D*, S3*D*, and S4). The expression level of YajC and YhcB, made with a single N-terminal TMS, was not found to be affected by the depletion of YidC (19). It is unknown if the biogenesis of SecG, which is topologically similar to F_0c with two TMS, depends on YidC. In these expression experiments, the control and experimental groups grew at similar rates, and their overall protein content

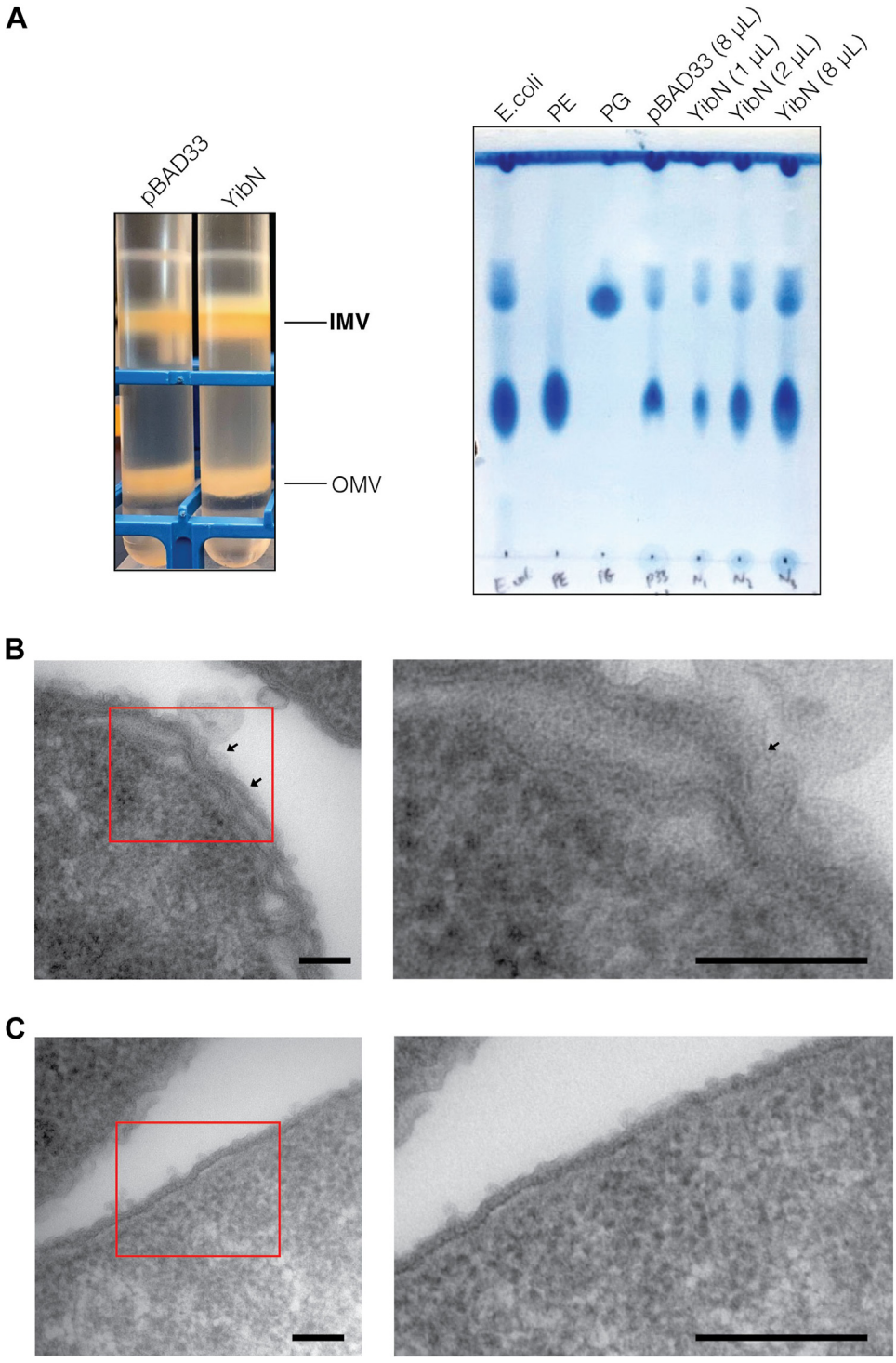

Figure 2. Membrane lipid analysis following YibN over-expression. *A*, inner and outer membrane isolation on sucrose gradient and lipid content analysis on thin layer chromatography (TLC). *Left panel*: IMV and OMV isolation of cells bearing either empty pBAD33 or pBAD33 YibN on 20-50 to 70% sucrose gradient. *Right panel*: TLC analysis of lipid extracts obtained from 30 µg of YibN overproduced inner membrane and 30 µg of control inner membrane. *B*, transmission electron micrographs of sectioned *E.coli* BL21 (DE3) with over-expressed YibN. BL21 (DE3) bearing YibN was grown at room temperature until OD_{600} reached 0.4. 0.1% arabinose was used to induce the overproduction of YibN. Cells continued to grow for another 1.5 h. *C*, A negative control, in which an empty vector was transformed and cells were grown and induced under the same condition as shown in (*B*). *Scale bar*, 100 nm. The *right panels* are the enlarged views of the area *circled* in *red* from the *left panels*.

was comparable (Fig. S3*D*). Interestingly, the biogenesis of YajC and YhcB was not affected by YibN (Fig. S4), but the biogenesis of SecG was significantly increased (left panel, Fig. 3*D*).

YibN stimulates protein insertion in vitro

To validate the YibN effect, we turned to an *in vitro* translation/insertion assay using inverted membrane vesicles (INVs) (30). Compared to the INVs prepared from the control

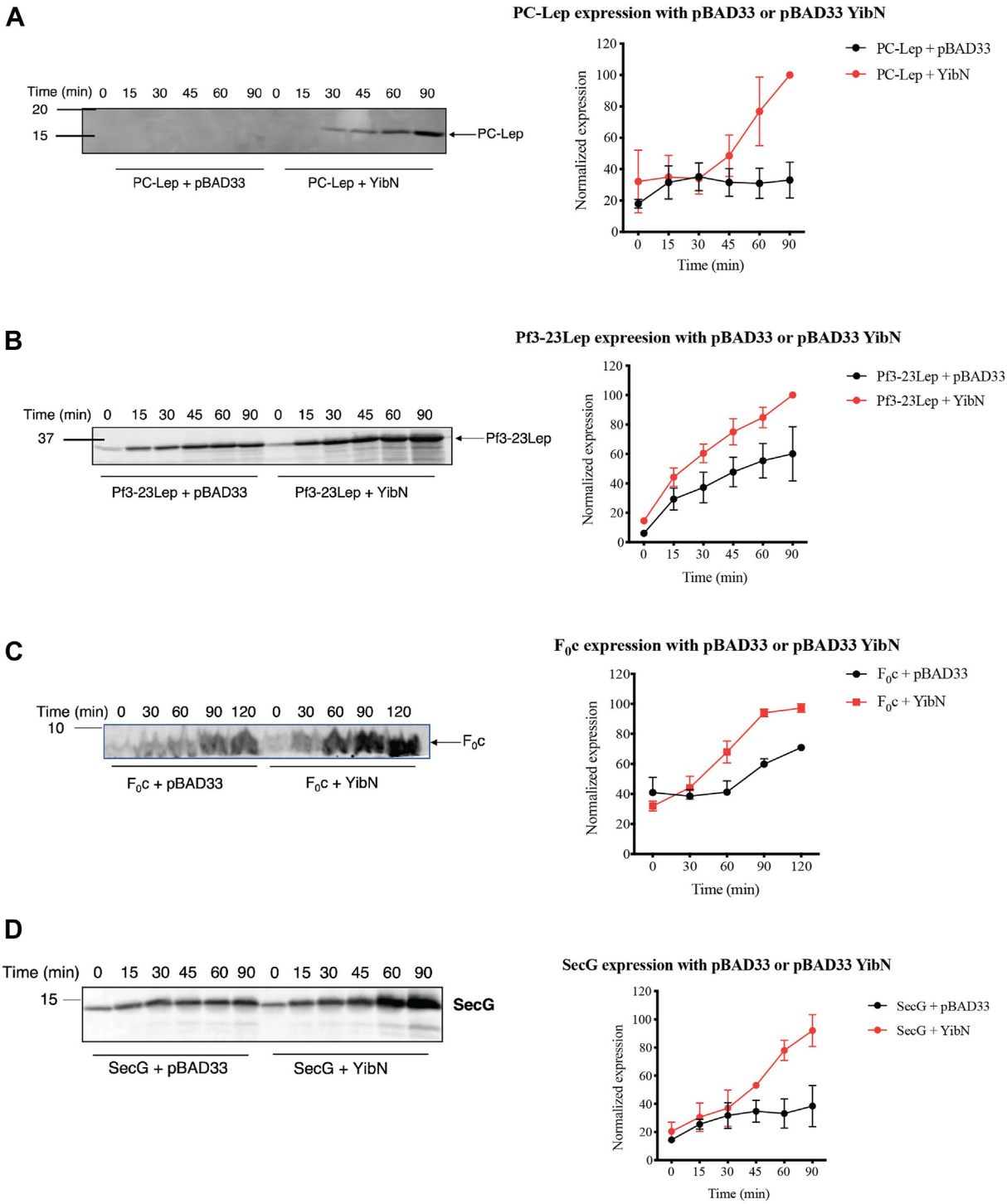

Figure 3. Effect of YibN on small membrane proteins biogenesis. *A*, PC-Lep, *B*, Pf3-23Lep, *C*, F_0c and *D*, SecG co-expression with empty pBAD33 or pBAD33 YibN at room temperature. The whole-cell lysates were analyzed by Western Blot (PC-Lep and Pf3-23Lep blots: anti-Lep antibody; F_0c blot: anti-F_0c antibody; SecG blot: anti-SecG antibody). The expression level of these small membrane proteins was quantified using ImageJ. The data represents the mean ± S.D. from the three independent experiments.

strain, INVs enriched for YibN supported a ∼1.5 to ∼1.8-fold stimulation of insertion of the substrates Pf3 coat, M13 procoat H5 and F_0c (Fig. 4). No such stimulation was obtained with INVs enriched for YidC, as previously reported (22). We also employed the SecG protein substrate. This protein is made with two TMS with N- and C-termini exposed to the periplasm but also exists in an inverted orientation, with its N- and C-termini exposed to the cytoplasm (Fig. S5) (31). After membrane insertion and proteinase K digestion, three membrane-protected fragments (MPF) were detected (*i.e.* MPF one and MPF two derived from normal SecG and one corresponding to the inverted SecG; Fig. 4, *D* and *E*). Their

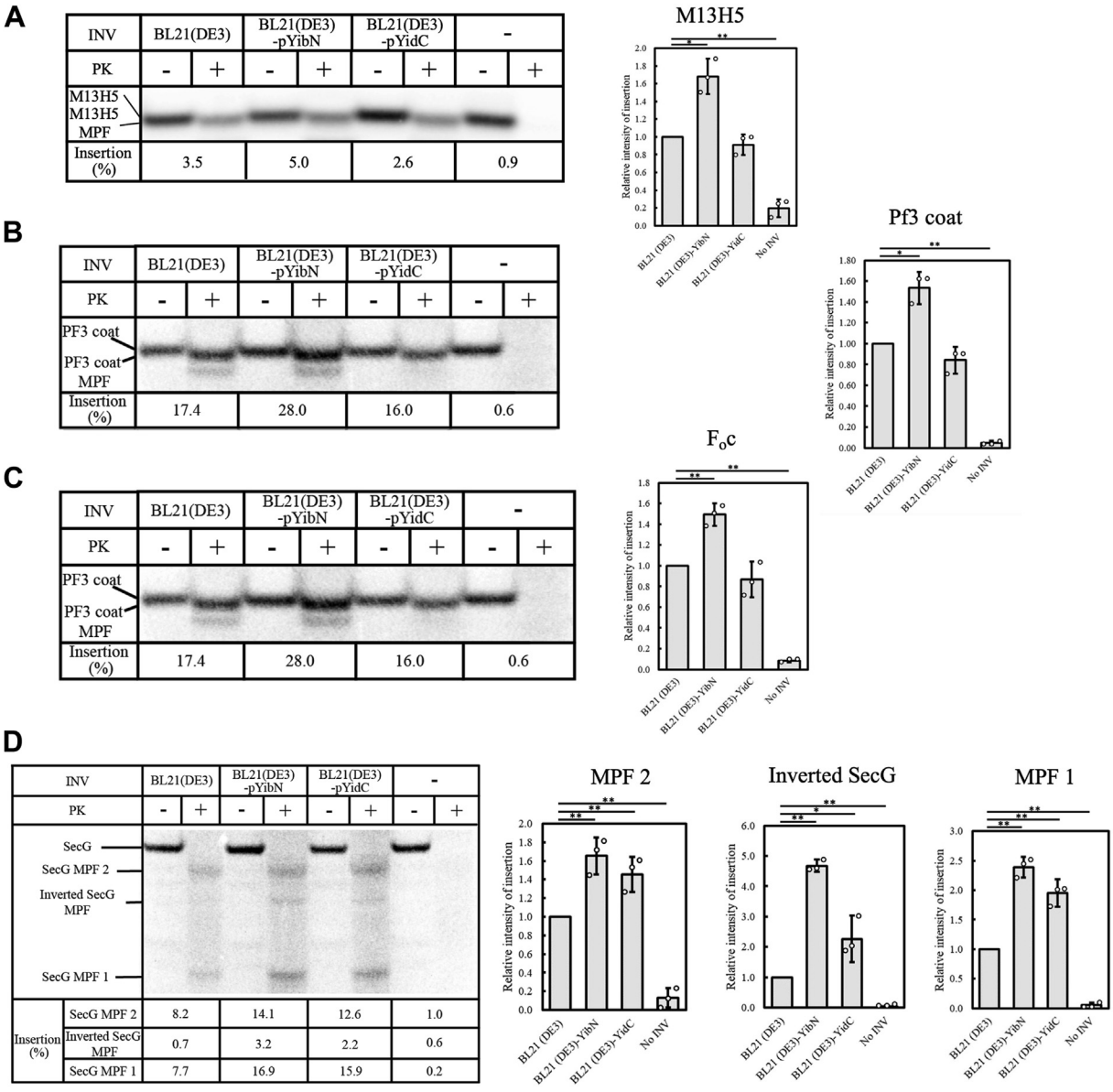

Figure 4. *In vitro* insertion assays of the small membrane proteins. *A*, M13 procoat, *B*, H5 Pf3 coat; *C*, F_0c and *D*, SecG were *in vitro* synthesized in the presence of wild-type INV (BL21(DE3)), YibN-overproduced INV (BL21(DE3)-pYibN) or YidC-overproduced INV (BL21(DE3)-pYidC) as described in "Experimental procedures". The control sample without INV was also set ('-' and 'No INV'). The membrane-inserted domain was generated by proteinase K (PK) digestion as a membrane-protected fragment (MPF). The insertion efficiency was calculated and expressed as a percentage of the translated level. The experiments were repeated at least three times. The relative activity of insertion to that in wild-type INV was shown with the SD values in graphs. Note that the full-length F_0c is given upon membrane insertion with PK digestion. In the case of SecG, three kinds of MPF (MPF2, inverted SecG, MPF1) are generated with PK digestion. Their activities relative to those in wild-type INV are shown with the SD values. The positions of each protein and MPFs is indicated.

quantitation showed MPF 1, MPF 2, as well as inverted SecG, are all augmented with INVs enriched for YibN, as much as that obtained using INVs enriched for YidC (Fig. 4*D*). Finally, we compared the Pf3 coat insertion using INVs prepared from the wild-type and *yibN* knockout strains, but no difference in membrane insertion efficiency was observed (Fig. S6), perhaps as a reflection of the non-essentiality of this gene in *E. coli* (Fig. S7).

Discussion

YidC belongs to the "Oxa1 superfamily", which includes the closely related Oxa1/Alb3 proteins and the functionally analogous EMC3, TMCO1, GET1, and Oxa1L insertion factors (32–35). These proteins typically feature a conserved structure characterized by a membrane-exposed hydrophilic groove that facilitates the translocation of membrane proteins into the lipid bilayer (36, 37). This structural groove is linked to a membrane bilayer thinning mechanism that probably reduces the energy expenditure required for the translocation process (38, 39). Additionally, this groove is implicated in inter-leaflet membrane lipid scramblase activity, a trait that also characterizes the membrane insertase family (25). This dual functionality highlights the importance these proteins have in maintaining membrane integrity while assisting in the

proper insertion and arrangement of other membrane proteins (33, 40, 41).

In *E. coli*, the common view is that YidC possesses structural elements enabling the protein to operate alone, although recent reports on the closely related Oxa1L identify TMEM126A as a specific interactor (35). In this study, we used BioID to probe the protein environment of YidC and found YibN - a previously uncharacterized inner membrane protein - to be highly proximal. Our SILAC-AP/MS experiments confirmed that YidC and YibN reciprocally capture each other (Fig. 1, *C* and *D*), with endogenous YibN enabling the enrichment of endogenous YidC (Fig. 1*E*). To validate this further, we purified these two proteins and applied an on-gel binding assay to find that YidC and YibN form a stable complex in detergent (Fig. 1*F*). The deletion of the YibN unique transmembrane segment abolished this association, implying that the hydrophobic region is critical for the stability of this complex and suggesting that the binary interaction likely occurs within the hydrophobic interior of the lipid bilayer. Collectively, the evidence supports the conclusion that YibN is a *bona fide* interactor of YidC, pointing to a possible role in membrane protein biogenesis.

YibN is a 16 kDa protein composed of an N-terminal transmembrane segment and a cytosolic rhodanese-like domain. The rhodanese-like domain is widely conserved across evolution. However, when considering the presence of the transmembrane segment, it emerges that YibN is conserved only in enterobacteria (>95% identity in sequence) and certain Gram-positive bacteria, such as *Bacillus subtilis* (46% identity). Interestingly, it was reported earlier that YibN is upregulated upon depletion of YidC or depletion of SecDF-YajC (19, 42), suggesting a possible involvement of YibN in the membrane protein biogenesis pathway. We note here that the gene *yibN* is located on the same operon as *grxC*, *secB*, and *gpsA* (43), which encode for proteins with physiological relationships. The protein GrxC promotes protein disulfide bond reduction, SecB maintains proteins competent for secretion, and GpsA is involved in glycerophospholipid synthesis (44–49). YibN, however, is not essential in *E. coli;* the knockout strain JW3586 does not display any obvious growth defects at the different temperatures tested (Fig. S7). This non-essentiality complicates the analysis since without evident defects, distinguishing the physiological and biochemical contributions of YibN becomes more challenging.

In our co-expression experiments, we observed that the production of YibN increases the production of the YidC substrates PC-Lep, Pf3-Lep, and F_0c (Fig. 3). YibN also augmented the production of SecG (Fig. 3*D*), but not YajC and YhcB, whose production was not reported affected by YidC depletion (19) (Fig. S4). To obtain additional experimental support, we turned to an *in vitro* translation and insertion assay (Fig. 4). The substrates PC-Lep, Pf3-23-Lep, F_0c and SecG all showed significant increased insertion using membranes enriched with YibN, whereas membranes enriched with YidC had less effect (Fig. 4). Studies have shown that YidC-dependent translocation is contingent on the MPIase glycolipid such that YidC overexpression would have less bearing on translocation insofar as MPIase level content remains constant (21, 22).

Interestingly, YibN expression induced noticeable membrane lipid production alteration and local cell surface deformation (Figs. 2 and S2). Studies have found that cells lacking membrane insertases exhibit defects in membrane morphology and lipid metabolism, which align with their role as glycerophospholipid scramblases ((24, 25, 50), and references within). We speculate herein that the overproduction of YibN could interfere with the YidC lipid transport activity. This interference may occur due to an imbalance in protein-protein interactions, potentially leading to the alteration of YidC's ability to scramble lipids. The mechanistic basis that underlies YibN's role in modulating YidC activity thus remains to be explored.

Experimental procedures

Strains and plasmids

The strains and plasmids used in this study are listed in Table S1. *E. coli* strain BL21 (DE3) was used for recombinant protein expression. All the constructs were made through the PIPE cloning method (51). The pAD22-$_{His}$YidC expression vector was obtained from our laboratory collection (52). The BirA gene was cloned from the *E. coli* genome into the pET28a vector, and a point mutation (R118G) was introduced to obtain BirA*. The pBAD22 YidC-BioID construct was obtained by fusing BirA* onto the C-terminus of $_{His6}$-YidC. All sequences (BirA, BirA*, and YidC-BioID) were confirmed through Sanger Sequencing.

Growth of YidC-BioID and membrane preparation

A single colony of BL21 (DE3) bearing pBAD22 YidC-BirA* plasmid was inoculated in a 10 ml overnight culture in LB media supplemented with 100 μg/ml ampicillin. The overnight culture was backdiluted 1/100 into 1 L fresh LB media supplemented with ampicillin and grown until OD_{600} ∼ 0.4. Protein expression was induced with 0.2% arabinose for another 2 h. Cells were harvested by centrifugation (6000*g*, 10 min) and resuspended in the TSG buffer (50 mM Tris pH 7.9, 100 mM NaCl, 10% glycerol) containing 1 mM PMSF. The cell lysate was obtained by passing the cells over a Microfluidizer (12,000 psi, three times). Unlysed cells were removed by centrifugation (3000*g*, 10 min). The crude membrane fraction was obtained by ultracentrifugation (100,000*g*, 45 min) in a Ti45 rotor. The crude membrane pellet was resuspended in 10 ml of TSG buffer. The inner and outer membrane fractions were further isolated through a step-sucrose gradient (20–50–70%) as previously described (53). The inner membrane fraction was collected from the 20 to 50% sucrose interface. The inner membrane fraction was diluted with TSG buffer and centrifuged again to remove the sucrose (TLA-110 rotor, 164,000*g*, 20 min). The inner membrane fraction was resuspended in the TSG buffer.

Biotinylated proteins enrichment assay

The YidC-BirA* inner membrane fraction (2 mg) was solubilized with 1% n-dodecyl-β-d-maltoside (DDM) for 1 h at 4 °C with gentle shaking. The insoluble material was removed by centrifugation (100,000*g*, 15 min). The DDM-extracted material was incubated with 120 μl NeutrAvidin resin equilibrated in the TSG buffer containing 0.02% DDM. The sample was then split into four fractions (each fraction containing ∼500 μg of solubilized material plus 30 μl NeutrAvidin resin). Fractions 1 and 2 (technical replicates) were washed with 1× PBS buffer (137 mM NaCl, 2.7 mM KCl, 10 mM Na_2HPO_4, 1.8 mM KH_2PO_4) (eight times, 500 μl each) with 0.02% DDM. Fraction three was washed with 1 M NaCl (four times, 500 μl each) supplemented with 0.02% DDM and then 1× PBS + 0.02% DDM buffer (four times, each time 500 μl). Fraction four was washed with 10% DMSO (four times, each time 500 μl) and then 1× PBS buffer (four times, each time 500 μl). The biotinylated proteins were eluted with a solution containing 80% acetonitrile, 0.2% trifluoroacetic acid (TFA), and 0.1% formic acid. The samples were then dried in SpeedVac and resuspended in 100 μl of 20 mM NH_4HCO_3 before trypsin digestion. The tryptic peptides were then Stage-tipped and analyzed on LC-MS/MS.

Expression of YidC and YibN in SILAC labeling conditions

Plasmids pBAD22, pBAD33, pBAD22 $_{His6}$-YidC and pBAD33-YibN-$_{His6}$ were transformed into *E. coli* JW2806 strain. SILAC labeling was performed as previously described (17). Briefly, cells were grown overnight in M9 media supplemented with either 0.3 mg/ml Lys4 ($^2H_4$-lysine, "heavy" pBAD22 $_{His6}$-YidC and pBAD33 YibN-$_{His6}$; the experimental group) or 0.3 mg/ml regular lysine Lys0 (regular lysine, "light" for pBAD22 and pBAD33; the control group). On the second day, cultures were backdiluted 1/100 into fresh M9 media supplemented with either Lys4 (experimental group) or Lys0 (control group). The cells were grown at 37 °C until OD_{600} ∼ 0.4 and induced with 0.02% arabinose. After growth at room temperature overnight (∼16 h), cells were harvested by centrifugation (3000*g*, 10 min). The cell pellets were resuspended in 4 ml of TSG buffer containing 1 mM PMSF. Following cell lysis on a French Press (500 psi, three passes), unlysed cells were removed through centrifugation (3000*g*, 10 min), and the supernatant was subject to ultracentrifugation (100,000*g*, 20 min) to obtain the membrane fraction.

Isolation of SILAC-labeled YidC and YibN

Membranes prepared from the "heavy" (pBAD22 $_{His6}$-YidC and pBAD33 YibN-$_{His6}$) and "light" (pBAD22 and pBAD33) conditions were solubilized with 0.5% DDM in TSG buffer at 4 °C with gentle shaking. The insoluble material was removed by ultracentrifugation (100,000*g*, 15 min) and the detergent-solubilized material (∼500 μg each) was incubated with Ni-NTA agarose beads at 4 °C for ∼2 h with gentle shaking. The resin was washed with the TS/DDM buffer (50 mM Tris, 100 mM NaCl, 0.02% DDM; 5 times, each time 1 ml). The proteins were eluted in TS/DDM buffer supplemented with 600 mM imidazole. The eluted proteins from the "heavy" pBAD22 $_{His6}$-YidC and "light" pBAD22 samples were pooled together. The eluted proteins from the "heavy" pBAD33 YibN-$_{His6}$, and "light" pBAD33 were pooled together. To remove detergents before MS analysis, the pooled samples were treated with 1 ml 100% ice-cold acetone and incubated overnight at −20 °C. The proteins were sedimented by centrifugation (16,100*g*, 10 min). The acetone was removed and the protein pellets were air-dried. The pellets were resuspended in 50 μl of 20 mM NH_4HCO_3 before trypsin digestion.

YibN-SPA membrane isolation and FLAG pull-down

The procedures for YibN-SPA cell growth, membrane isolation and membrane solubilization were described in Young *et al.*, 2022 (7). Briefly, strain B3611 (chromosomal expression of SPA-tagged YibN) and strain DY330 (control) were revived on LB-agar plates with/without Kanamycin antibiotic. A single colony was inoculated for overnight growth and back-diluted 1/100 into fresh LB media at 37 °C until the OD_{600} ∼ 1. Cells were harvested and lysed as described above. The membrane fraction was isolated by ultracentrifugation (100,000*g*, 30 min) followed by resuspension in the TSG buffer. The membrane fraction was solubilized in 0.5% DDM. The detergent extract (∼1 mg) was incubated with 50 μl of ANTI-FLAG M2 affinity gel at 4 °C overnight with gentle shaking. The resin was washed with TSG-DDM buffer (50 mM Tris, pH 7.8; 100 mM NaCl; 10% glycerol; 0.02% DDM) 6 times. Bound proteins were eluted in 100 mM Glycine HCl, pH 3.5. The pH was then adjusted to 8.0 with 1 M Tris, pH 8. The proteins were precipitated in acetone to remove detergent, as described above.

MS sample preparation and analysis

The samples described above (YidC-BioID, YidC-SILAC-AP, YibN-SILAC-AP, and YibN-SPA) were treated with 6 M urea for 30 min at room temperature. Samples were treated with 10 mM DTT for 1 h and with 20 mM IAA for another 30 min 10 mM DTT was further added to the samples for 30 min. The samples were then diluted 5 times with the TS buffer (50 mM Tris, pH 7.8; 100 mM NaCl) and trypsin-Gold was added at an enzyme-to-protein ratio of 1:50 for 16 h. The tryptic peptides were Stage-tipped and dried in SpeedVac. Data were acquired on a Bruker Daltonics Impact II quadrupole time-of-flight mass spectrometer connected online to an easy nLC-1000 HPLC (Thermo Scientific). A one-column set up was utilized and peptides were separated using a 35 cm, 75 μm I.D. column packed with 1.8 μm C18 resin (Dr Maisch). Peptides were loaded onto the column using buffer A alone (0.1% formic acid in water) at 800 bar for a total of 5 μl volume washed and then eluted on a linear gradient from 2% buffer B (0.1% formic acid in acetonitrile) to 35% buffer B in 60 min then washed with 90% buffer B for 10 min. The Impact II mass spectrometer was operated in data-dependent acquisition mode with a top20 method. MS1 scans were measured at 5 Hz and collision-induced dissociation (CID) performed on the 20

most intense ions between charge states two and 6. Each MS/MS event was done at a scan rate of 20 Hz and excluded for 30 s unless the intensity of the precursor was 4× greater than its previous MS/MS event. Data were then processed with DataAnalysis to convert files into.mgf files.

All MS/MS samples (mgf files) were analyzed using Mascot (Matrix Science, London, UK; version 2.5.1). Mascot was set up to search the *E. coli* K12 (accessed May 12 2016) database (8612 entries) assuming the digestion enzyme trypsin. Mascot was searched with a fragment ion mass tolerance of 0.100 Da and a parent ion tolerance of 50 PPM. Carbamidomethylation of cysteine (+57.021464 Da) was specified in Mascot as a fixed modification. Oxidation of methionine (+15.99491 Da) and biotinylation of lysine and the N-terminus (+226.077598 Da) were specified in Mascot as variable modifications.

Scaffold (version Scaffold 4.8.5, Proteome Software Inc., Portland, OR) was used to validate MS/MS based peptide and protein identifications. Peptide identifications were accepted if they could be established at greater than 98.0% probability to achieve an FDR less than 1.0%. Peptide Probabilities from Mascot were assigned by the Scaffold Local FDR algorithm. Protein identifications were accepted if they could be established at greater than 84.0% probability to achieve an FDR less than 1.0% and contain at least one identified peptide. Protein probabilities were assigned by the Protein Prophet algorithm (54). Proteins that contained similar peptides and could not be differentiated based on MS/MS analysis alone were grouped to satisfy the principles of parsimony. Spectral counts for identified proteins were determined through Scaffold and used to estimate the relative abundance of proteins.

Quantitative analysis of SILAC-labeled samples: Raw files from the Impact II MS system (.d folders) were searched directly with Maxquant. Quantitative modifications used ^{15}N labeling for analysis, fixed modification of carbamidomethylation of cysteine (+57.021464 Da), and variable modifications: oxidation of methionine (+15.99491 Da) and biotinylation of lysine and the N-terminus (+226.077598 Da) (if for BioID experiment). Peptide and protein FDRs were set to 1% and results later imported and analyzed in the Perseus software environment.

YidC, YibN, and YibNΔ1 to 29 purification and binding assay

Plasmids pBAD22 $_{His6}$-YidC, pBAD33 YibN-$_{His6}$, and pBAD33 YibNΔ1 to 29-$_{His6}$ were transformed into BL21 (DE3) strain. The procedures to grow cells and isolate membranes of $_{His6}$-YidC and YibN (full length) were as described above (section "Growth of YidC-BioID and membrane preparation"). The protein expression was verified by loading aliquots of the membrane and soluble fractions on a 15% SDS-PAGE followed by Coomassie blue staining. Membranes were solubilized with 1% DDM for 1 h at 4 °C with gentle shaking. The insoluble material was removed by centrifugation (100,000*g*, 15 min). The detergent extract or cytosolic fraction (∼8 mg each) was passed through a Ni-NTA gravity column (1 ml resin). The flowthrough was collected, and the resin was washed with 50 ml TSG-DDM buffer plus 20 mM imidazole. Bound proteins were then eluted with TSG-DDM buffer supplemented with 600 mM imidazole. Purified YidC (3 μg) was incubated with either purified YibN or purified YibN Δ1 to 29 (3 μg each) for 15 min on ice. The protein samples were then analyzed by Blue Native-PAGE and 15% SDS-PAGE.

BW25113 and JW3586 growth at various temperatures

A single colony of strains BW25113 (no antibiotic) and JW3586 (25 μg/ml Kanamycin) was inoculated and grown in LB media overnight, respectively. On the second day, based on the OD_{600} reading, a similar number of cells were back diluted 1/50 into fresh LB media with no antibiotics. The cells were grown at 18 °C, 37 °C or 42 °C for 3 h. Later, two strains were plated on LB agar plates and the cells were recovered at 37 °C. A serial dilution with a dilution factor of 10 was performed.

Co-expression of YibN with the YidC substrates PC-Lep, Pf3-Lep, F_0c and SecG

Plasmids pMS119 PC-Lep, pMS119 Pf3-Lep, pET20 *atpE* (encoding F_0c) and pBAD22 SecG were co-transformed with either empty vector pBAD33 (control) or pBAD33 YibN plasmid (experimental group) into strain BL21 (DE3). For each co-transformant, a single colony was inoculated into 10 ml LB media plus 10 μg/ml Ampicillin and 30 μg/ml Chloramphenicol antibiotics and grown overnight at 37 °C. On the second day, the overnight cultures were back diluted 1/100 into fresh LB media with antibiotics. The cells were grown at room temperature until their OD_{600} reached 0.4. For the co-expression of pBAD22 SecG with empty pBAD33 or with pBAD33 YibN, 0.1% arabinose was used for protein induction. The cells continued to grow for another 1.5 h. For the co-expression of pMS119 PC-Lep, pMS119 Pf3-Lep, and pET20 *atpE* with empty pBAD33 or with pBAD33 YibN, the cells were firstly induced with 0.1% arabinose for 15 min. The cells were then induced with 0.75 mM Isopropyl β-D-1-thiogalactopyranoside (IPTG) for another 1.5 to 2 h. Time-course aliquots were taken and analyzed by SDS-PAGE and Western Blot.

In vitro *membrane protein insertion assay*

BL21(DE3) and BL21(DE3) carrying plasmid pBAD33 YibN or pBAD22 YidC were cultivated in LB medium at 25 °C. At the mid-log phase, 0.2% arabinose was added to express YibN and YidC, respectively. After cultivation was continued for 3 h, INV (inverted membrane vesicles) were prepared as described (55) and then subjected to the insertion assay *in vitro*. The reaction mixture (20 μl) was composed of the pure system, a reconstituted translation system (56), INV (0.5 mg protein/ml), plasmid DNA in which the substrate membrane proteins are encoded under the control of the T7 promoter (50 μg/ml), and [^{35}S] methionine and cysteine (∼10 MBq/ml). When SecG insertion was analyzed, SecA (60 μg/ml) was additionally included. INV was added to the mixture 10 min after the start of the reaction. The translation/insertion reaction was allowed to proceed at 25 °C for 90 min. The reaction was then terminated by chilling the mixture in ice. An aliquot (3 μl) was

treated with 5% trichloroacetic acid (TCA) to monitor the translation level. The other aliquot (15 µl) was digested with proteinase K (0.5 mg/ml) to generate the membrane-protected fragments (MPF) as an index of membrane insertion, followed by TCA (5%) precipitation. The proteins were then analyzed by SDS-PAGE and autoradiography, as described (56). The radioactive bands were visualized by Phosphorimager (Typhoon, GE). The individual bands were quantified using the ImageQuant software (GE).

Lipid extraction and TLC

Purified inner membranes (30 µg) with YibN overexpressed or control (empty vector) were diluted to a final volume of 200 µl in TSG buffer. The diluted membrane was then mixed with 800 µl of methanol: chloroform solution (2:1 vol/vol). After 15 min at room temperature, 200 µl of chloroform and 200 µl of dH_2O were added sequentially to the samples and mixed briefly. The two phases were separated by centrifugation at 3000 × rpm for 10 min. The organic phase, which contains lipids, was dried under nitrogen. The dried lipids were resuspended in 30 µl of chloroform and spotted onto a TLC Silica gel (Millipore). The TLC plate was developed in a solution composed of 35:25:3:28 (vol:vol) of chlorofrom:-triethylamine:dH_2O:ethanol. Plates were air dried and Coomassie stained (57).

Transmission electron microscopy

A single colony of BL21 bearing pBAD33-YibN or empty pBAD33 plasmid was picked to inoculate in a 10 ml overnight culture in LB media supplemented with 30 µg/ml chloramphenicol. The overnight culture was backdiluted 1/100 into 10 ml fresh LB media supplemented with chloramphenicol and grown until OD_{600} reached 0.4. Both cultures (BL21 pBAD33 YibN and BL21 pBAD33) were induced with 0.2% arabinose for another 2 h. Cells were harvested by centrifugation (6000*g*, 10 min). Cell pellets (10 µl) obtained from BL21 pBAD33 YibN and BL21 pBAD33 were treated with a fixative buffer (2.5% glutaraldehyde, 4% formaldehyde, and 0.1 M sodium cacodylate, pH 6.9), then washed with 0.1 M sodium cacodylate buffer. The cells were then fixed with 1% osmium tetroxide and rinsed with water. Staining was performed with 2% uranyl acetate and the cell pellets were rinsed with water and dehydrated by ethanol. The dehydrated cells were transferred and embedded into Epon Resin. After resin polymerization, thin sections were cut and adsorbed onto electron grids. The samples were visualized under Tecnai Spirit TEM.

Data availability

The datasets generated during and/or analyzed during the current study are available from the corresponding author on reasonable request.

Supporting information—This article contains supporting information.

Acknowledgments—We are thankful to Dr Ross Dalbey's lab for the gift of plasmids PC-Lep and Pf3-23Lep, and Dr rer. nat. Gabriele Deckers-Hebestreit for the plasmid pET20 atpE and the anti-F_0c antibody. We acknowledge the UBC Bioimaging Facility (RRID: SCR_021304) for the Tecnai Spirit TEM data.

Author contributions—F. D. H., M. A., Z. Z., and K. N. writing – review & editing; F. D. H. and M. B project administration; F. D. H., A. F., S. K., H. A., H. L., C. O., N. Y., and N. S. methodology; F. D. H., A. F., H. L., Z. Z., N. Y., K. N., and J. Y. investigation; F. D. H., M. A., H. A., Z. Z., N. Y., K. N., and J. Y. conceptualization; A. F., Z. Z., N. Y., and J. Y. formal analysis; S. K., H. A., S. P., Z. Z., H. N., N. Y., J. Y., and N. S. data curation; S. P. software; C. O. and K. N. supervision; Z. Z. and N. Y. Writing – original draft; M. B. supervision; M. B. and K. N. funding acquisition.

Funding and additional information—The work was supported by the Natural Sciences and Engineering Research Council of Canada (DG AWD-008949 to FDvH and DG-20234 to M. B.), the Canadian Institutes for Health Research (FDN-148408 to C. M. O.), and the Japan Society for the Promotion of Science (KAKENHI 24H01107, 23H04536, 22H02567 to K.-i. N.). C. M. O. is a Canada Research Chair.

Conflict of interest—The authors declare that they have no conflicts of interest with the contents of this article.

Abbreviations—The abbreviations used are: BioID, proximity-dependent biotin labeling; F0c, F_1F_0 ATP synthase subunit c; MPs, Membrane proteins; PE, phosphatidylethanolamine; PG, phosphatidylglycerol.

References

1. Lodish, H., Berk, A., Kaiser, C. A., Krieger, M., Scott, M. P., and Zipursky, S. L. (2000) *Molecular Cell Biology*, 4th Ed., Freeman & Co, Houndsmills, UK
2. Wickner, W., Leonard, M. R., and Economou, A. (1995) On the road to translocase. *Cold Spring Harb. Symp. Quant. Biol.* **60**, 285–290
3. Rapoport, T. A., Li, L., and Park, E. (2017) Structural and mechanistic insights into protein translocation. *Annu. Rev. Cell Dev. Biol.* **33**, 369–390
4. du Plessis, D. J. F., Nouwen, N., and Driessen, A. J. M. (2011) The Sec translocase. *Biochim. Biophys. Acta* **1808**, 851–865
5. Corey, R. A., Allen, W. J., and Collinson, I. (2016) Protein translocation: what's the problem? *Biochem. Soc. Trans.* **44**, 753–759
6. Oswald, J., Njenga, R., Natriashvili, A., Sarmah, P., and Koch, H.-G. (2021) The dynamic SecYEG translocon. *Front. Mol. Biosci.* **8**, 664241
7. Young, J. W., Wason, I. S., Zhao, Z., Kim, S., Aoki, H., Phanse, S., *et al.* (2022) Development of a method combining peptidiscs and proteomics to identify, stabilize, and purify a detergent-sensitive membrane protein assembly. *J. Proteome Res.* **21**, 1748–1758
8. Kuhn, A., Koch, H.-G., and Dalbey, R. E. (2017) Targeting and insertion of membrane proteins. *EcoSal Plus*. https://doi.org/10.1128/ecosalplus.ESP-0012-2016
9. Serdiuk, T., Steudle, A., Mari, S. A., Manioglu, S., Kaback, H. R., Kuhn, A., *et al.* (2019) Insertion and folding pathways of single membrane proteins guided by translocases and insertases. *Sci. Adv.* **5**, eaau6824
10. Hennon, S. W., Soman, R., Zhu, L., and Dalbey, R. E. (2015) YidC/Alb3/Oxa1 family of insertases. *J. Biol. Chem.* **290**, 14866–14874
11. McDowell, M. A., Heimes, M., and Sinning, I. (2021) Structural and molecular mechanisms for membrane protein biogenesis by the Oxa1 superfamily. *Nat. Struct. Mol. Biol.* **28**, 234–239
12. Chen, M., Samuelson, J. C., Jiang, F., Muller, M., Kuhn, A., and Dalbey, R. E. (2002) Direct interaction of YidC with the Sec-independent Pf3 coat protein during its membrane protein insertion. *J. Biol. Chem.* **277**, 7670–7675

13. van der Laan, M., Bechtluft, P., Kol, S., Nouwen, N., and Driessen, A. J. M. (2004) F1F0 ATP synthase subunit c is a substrate of the novel YidC pathway for membrane protein biogenesis. *J. Cell Biol.* **165**, 213–222
14. Facey, S. J., Neugebauer, S. A., Krauss, S., and Kuhn, A. (2007) The mechanosensitive channel protein MscL is targeted by the SRP to the novel YidC membrane insertion pathway of Escherichia coli. *J. Mol. Biol.* **365**, 995–1004
15. Aschtgen, M.-S., Zoued, A., Lloubès, R., Journet, L., and Cascales, E. (2012) The C-tail anchored TssL subunit, an essential protein of the enteroaggregative Escherichia coli Sci-1 Type VI secretion system, is inserted by YidC. *Microbiologyopen* **1**, 71–82
16. Babu, M., Butland, G., Pogoutse, O., Li, J., Greenblatt, J. F., and Emili, A. (2009) Sequential peptide affinity purification system for the systematic isolation and identification of protein complexes from Escherichia coli. *Methods Mol. Biol.* **564**, 373–400
17. Carlson, M. L., Stacey, R. G., Young, J. W., Wason, I. S., Zhao, Z., Rattray, D. G., *et al.* (2019) Profiling the Escherichia coli membrane protein interactome captured in Peptidisc libraries. *Elife*. https://doi.org/10.7554/eLife.46615
18. van Bloois, E., Dekker, H. L., Fröderberg, L., Houben, E. N. G., Urbanus, M. L., de Koster, C. G., *et al.* (2008) Detection of cross-links between FtsH, YidC, HflK/C suggests a linked role for these proteins in quality control upon insertion of bacterial inner membrane proteins. *FEBS Lett.* **582**, 1419–1424
19. Wickström, D., Wagner, S., Simonsson, P., Pop, O., Baars, L., Ytterberg, A. J., *et al.* (2011) Characterization of the consequences of YidC depletion on the inner membrane proteome of E. coli using 2D blue native/SDS-PAGE. *J. Mol. Biol.* **409**, 124–135
20. Nishiyama, K., Maeda, M., Yanagisawa, K., Nagase, R., Komura, H., Iwashita, T., *et al.* (2012) MPIase is a glycolipozyme essential for membrane protein integration. *Nat. Commun.* **3**, 1260
21. Sasaki, M., Nishikawa, H., Suzuki, S., Moser, M., Huber, M., Sawasato, K., *et al.* (2019) The bacterial protein YidC accelerates MPIase-dependent integration of membrane proteins. *J. Biol. Chem.* **294**, 18898–18908
22. Endo, Y., Shimizu, Y., Nishikawa, H., Sawasato, K., and Nishiyama, K.-I. (2022) Interplay between MPIase, YidC, and PMF during Sec-independent insertion of membrane proteins. *Life Sci. Alliance*. https://doi.org/10.26508/lsa.202101162
23. Roux, K. J., Kim, D. I., Raida, M., and Burke, B. (2012) A promiscuous biotin ligase fusion protein identifies proximal and interacting proteins in mammalian cells. *J. Cell Biol.* **196**, 801–810
24. Bartoš, L., Menon, A. K., and Vácha, R. (2024) Insertases scramble lipids: molecular simulations of MTCH2. *Structure* **32**, 505–510.e4
25. Li, D., Rocha-Roa, C., Schilling, M. A., Reinisch, K. M., and Vanni, S. (2024) Lipid scrambling is a general feature of protein insertases. *Proc. Natl. Acad. Sci. U. S. A.* **121**, e2319476121
26. Babu, M., Bundalovic-Torma, C., Calmettes, C., Phanse, S., Zhang, Q., Jiang, Y., *et al.* (2018) Global landscape of cell envelope protein complexes in Escherichia coli. *Nat. Biotechnol.* **36**, 103–112
27. Zeghouf, M., Li, J., Butland, G., Borkowska, A., Canadien, V., Richards, D., *et al.* (2004) Sequential Peptide Affinity (SPA) system for the identification of mammalian and bacterial protein complexes. *J. Proteome Res.* **3**, 463–468
28. Zhu, L., Wasey, A., White, S. H., and Dalbey, R. E. (2013) Charge composition features of model single-span membrane proteins that determine selection of YidC and SecYEG translocase pathways in Escherichia coli. *J. Biol. Chem.* **288**, 7704–7716
29. Soman, R., Yuan, J., Kuhn, A., and Dalbey, R. E. (2014) Polarity and charge of the periplasmic loop determine the YidC and sec translocase requirement for the M13 procoat lep protein. *J. Biol. Chem.* **289**, 1023–1032
30. Nishikawa, H., Sasaki, M., and Nishiyama, K.-I. (2020) *In vitro* assay for bacterial membrane protein integration into proteoliposomes. *Bio Protoc.* **10**, e3626
31. Nishiyama, K., Suzuki, T., and Tokuda, H. (1996) Inversion of the membrane topology of SecG coupled with SecA-dependent preprotein translocation. *Cell* **85**, 71–81
32. Anghel, S. A., McGilvray, P. T., Hegde, R. S., and Keenan, R. J. (2017) Identification of Oxa1 homologs operating in the eukaryotic endoplasmic reticulum. *Cell Rep.* **21**, 3708–3716
33. Hegde, R. S., and Keenan, R. J. (2022) The mechanisms of integral membrane protein biogenesis. *Nat. Rev. Mol. Cell Biol.* **23**, 107–124
34. Güngör, B., Flohr, T., Garg, S. G., and Herrmann, J. M. (2022) The ER membrane complex (EMC) can functionally replace the Oxa1 insertase in mitochondria. *PLoS Biol.* **20**, e3001380
35. Poerschke, S., Oeljeklaus, S., Cruz-Zaragoza, L. D., Schenzielorz, A., Dahal, D., Hillen, H. S., *et al.* (2024) Identification of TMEM126A as OXA1L-interacting protein reveals cotranslational quality control in mitochondria. *Mol. Cell* **84**, 345–358.e5
36. Kumazaki, K., Kishimoto, T., Furukawa, A., Mori, H., Tanaka, Y., Dohmae, N., *et al.* (2014) Crystal structure of Escherichia coli YidC, a membrane protein chaperone and insertase. *Sci. Rep.* **4**, 7299
37. Chen, Y., Sotomayor, M., Capponi, S., Hariharan, B., Sahu, I. D., Haase, M., *et al.* (2022) A hydrophilic microenvironment in the substrate-translocating groove of the YidC membrane insertase is essential for enzyme function. *J. Biol. Chem.* **298**, 101690
38. Wu, X., and Rapoport, T. A. (2021) Translocation of proteins through a distorted lipid bilayer. *Trends Cell Biol.* **31**, 473–484
39. Hegde, R. S., and Keenan, R. J. (2024) A unifying model for membrane protein biogenesis. *Nat. Struct. Mol. Biol.* **31**, 1009–1017
40. Vögtle, F.-N., Koch, H.-G., and Meisinger, C. (2022) A common evolutionary origin reveals fundamental principles of protein insertases. *PLoS Biol.* **20**, e3001558
41. Wang, Y., and Kinoshita, T. (2023) The role of lipid scramblases in regulating lipid distributions at cellular membranes. *Biochem. Soc. Trans.* **51**, 1857–1869
42. Young, J. W., Wason, I. S., Zhao, Z., Rattray, D. G., Foster, L. J., and Duong Van Hoa, F. (2020) His-tagged peptidiscs enable affinity purification of the membrane proteome for downstream mass spectrometry analysis. *J. Proteome Res.* **19**, 2553–2562
43. Seoh, H. K., and Tai, P. C. (1999) Catabolic repression of secB expression is positively controlled by cyclic AMP (cAMP) receptor protein-cAMP complexes at the transcriptional level. *J. Bacteriol.* **181**, 1892–1899
44. Prinz, W. A., Aslund, F., Holmgren, A., and Beckwith, J. (1997) The role of the thioredoxin and glutaredoxin pathways in reducing protein disulfide bonds in the Escherichia coli cytoplasm. *J. Biol. Chem.* **272**, 15661–15667
45. Diao, L., Dong, Q., Xu, Z., Yang, S., Zhou, J., and Freudl, R. (2012) Functional implementation of the posttranslational SecB-SecA protein-targeting pathway in Bacillus subtilis. *Appl. Environ. Microbiol.* **78**, 651–659
46. Sala, A., Bordes, P., and Genevaux, P. (2014) Multitasking SecB chaperones in bacteria. *Front. Microbiol.* **5**, 666
47. Eismann, L., Fijalkowski, I., Galmozzi, C. V., Koubek, J., Tippmann, F., Van Damme, P., *et al.* (2022) Selective ribosome profiling reveals a role for SecB in the co-translational inner membrane protein biogenesis. *Cell Rep.* **41**, 111776
48. Parsons, J. B., and Rock, C. O. (2013) Bacterial lipids: metabolism and membrane homeostasis. *Prog. Lipid Res.* **52**, 249–276
49. Drecktrah, D., Hall, L. S., Crouse, B., Schwarz, B., Richards, C., Bohrnsen, E., *et al.* (2022) The glycerol-3-phosphate dehydrogenases GpsA and GlpD constitute the oxidoreductive metabolic linchpin for Lyme disease spirochete host infectivity and persistence in the tick. *PLoS Pathog.* **18**, e1010385
50. Thompson, K., Mai, N., Oláhová, M., Scialó, F., Formosa, L. E., Stroud, D. A., *et al.* (2018) OXA1L mutations cause mitochondrial encephalopathy and a combined oxidative phosphorylation defect. *EMBO Mol. Med.* https://doi.org/10.15252/emmm.201809060
51. Klock, H. E., and Lesley, S. A. (2009) The Polymerase Incomplete Primer Extension (PIPE) method applied to high-throughput cloning and site-directed mutagenesis. *Methods Mol. Biol.* **498**, 91–103
52. Zhang, X. X., Chan, C. S., Bao, H., Fang, Y., Foster, L. J., and Duong, F. (2012) Nanodiscs and SILAC-based mass spectrometry to identify a membrane protein interactome. *J. Proteome Res.* **11**, 1454–1459

53. Cian, M. B., Giordano, N. P., Mettlach, J. A., Minor, K. E., and Dalebroux, Z. D. (2020) Separation of the cell envelope for gram-negative bacteria into inner and outer membrane fractions with technical adjustments for acinetobacter baumannii. *J. Vis. Exp.* https://doi.org/10.3791/60517
54. Nesvizhskii, A. I., Keller, A., Kolker, E., and Aebersold, R. (2003) A statistical model for identifying proteins by tandem mass spectrometry. *Anal. Chem.* **75**, 4646–4658
55. Alami, M., Trescher, D., Wu, L.-F., and Müller, M. (2002) Separate analysis of twin-arginine translocation (Tat)-specific membrane binding and translocation in Escherichia coli. *J. Biol. Chem.* **277**, 20499–20503
56. Nishiyama, K., Maeda, M., Abe, M., Kanamori, T., Shimamoto, K., Kusumoto, S., *et al.* (2010) A novel complete reconstitution system for membrane integration of the simplest membrane protein. *Biochem. Biophys. Res. Commun.* **394**, 733–736
57. Hofmann, T., Barth, M., Annette, M., Panagiotis, L., and Kastritis, C. S. (2021) Thin-layer chromatography and Coomassie staining of phospholipids for fast and simple lipidomics sample preparation. *Anal. Sens.* **1**, 171–179
58. Sachelaru, I., Winter, L., Knyazev, D. G., Zimmermann, M., Vogt, A., Kuttner, R., *et al.* (2017) YidC and SecYEG form a heterotetrameric protein translocation channel. *Sci. Rep.* **7**, 101